PROCEEDINGS B

rspb.royalsocietypublishing.org

Research

Cite this article: DeCarlo TM, Comeau S, Cornwall CE, McCulloch MT. 2018 Coral resistance to ocean acidification linked to increased calcium at the site of calcification. *Proc. R. Soc. B* **285**: 20180564.
http://dx.doi.org/10.1098/rspb.2018.0564

Received: 13 March 2018
Accepted: 9 April 2018

Subject Category:
Global change and conservation

Subject Areas:
environmental science

Keywords:
coral, calcification, ocean acidification, calcium

Author for correspondence:
T. M. DeCarlo
e-mail: thomas.decarlo@uwa.edu.au

†Present address: Sorbonne Université, CNRS-INSU, Laboratoire d'Océanographie de Villefranche, 181 chemin du Lazaret, F-06230 Villefranche-sur-mer, France.
‡Present address: School of Biological Sciences, Victoria University of Wellington, Wellington, New Zealand.

Electronic supplementary material is available online at https://dx.doi.org/10.6084/m9.figshare.c.4068788.

THE ROYAL SOCIETY PUBLISHING

Coral resistance to ocean acidification linked to increased calcium at the site of calcification

T. M. DeCarlo[1,2], S. Comeau[1,2,†], C. E. Cornwall[1,2,‡] and M. T. McCulloch[1,2]

[1]Oceans Institute and Oceans Graduate School, and [2]ARC Centre of Excellence for Coral Reef Studies, The University of Western Australia, 35 Stirling Hwy, Crawley, Western Australia 6009, Australia

TMD, 0000-0003-3269-1320; SC, 0000-0002-6724-5286; CEC, 0000-0002-6154-4082

Ocean acidification threatens the persistence of biogenic calcium carbonate ($CaCO_3$) production on coral reefs. However, some coral genera show resistance to declines in seawater pH, potentially achieved by modulating the chemistry of the fluid where calcification occurs. We use two novel geochemical techniques based on boron systematics and Raman spectroscopy, which together provide the first constraints on the sensitivity of coral calcifying fluid calcium concentrations ($[Ca^{2+}]_{cf}$) to changing seawater pH. In response to simulated end-of-century pH conditions, *Pocillopora damicornis* increased $[Ca^{2+}]_{cf}$ to as much as 25% above that of seawater and maintained constant calcification rates. Conversely, *Acropora youngei* displayed less control over $[Ca^{2+}]_{cf}$, and its calcification rates strongly declined at lower seawater pH. Although the role of $[Ca^{2+}]_{cf}$ in driving calcification has often been neglected, increasing $[Ca^{2+}]_{cf}$ may be a key mechanism enabling more resistant corals to cope with ocean acidification and continue to build $CaCO_3$ skeletons in a high-CO_2 world.

1. Introduction

Since the start of the industrial era, atmospheric CO_2 concentrations have increased from approximately 280 to over 400 ppmv today, primarily due to burning of fossil fuels and deforestation [1]. Although CO_2 levels in the geologic past (e.g. during the Eocene) were likely several times higher than today, it is the speed of CO_2 rise that dictates the severity of ocean acidification [2,3], with the current rate of CO_2 released by human activities being unprecedented even over million-year timescales [4]. However, despite its rapid rise, more than one quarter of anthropogenic CO_2 emissions have already been absorbed by the oceans [5], causing declines in seawater pH and hence aragonite saturation state ($\Omega_{Ar} = [CO_3^{2-}][Ca^{2+}]/K_{sp}$). Shallow-water coral reefs, which are found only within a relatively narrow range of open-ocean $\Omega_{Ar} > 3$ conditions [6], are likely to be among the most sensitive marine ecosystems to ocean acidification [6–8]. Under 'business-as-usual' CO_2 emissions, climate models project that the surface open ocean could be devoid of regions with $\Omega_{Ar} > 3$ by the end of the twenty-first century [9], potentially driving a rapid decline of corals and the calcium carbonate ($CaCO_3$)-based reef ecosystems that they build.

Crucial to interpreting the sensitivity of corals to ocean acidification is the mechanism by which calcification occurs. Scleractinian corals transport seawater to a micro-scale internal calcifying space [10–12], thereby supplying some of the calcium (Ca^{2+}) and carbonate (CO_3^{2-}) ions needed to build their aragonitic ($CaCO_3$) skeletons. However, as seawater pH declines, the concentration of carbonate ions ($[CO_3^{2-}]$) in seawater decreases, making precipitation of $CaCO_3$ less favourable due to lower Ω_{Ar} [13]. In laboratory experiments, many corals repeatedly show decreased calcification rates in response to lower-Ω_{Ar} conditions achieved by manipulating seawater pH or, less commonly, $[Ca^{2+}]$ [14–17]. Yet, it is increasingly recognized that not all corals are affected equally. Some species are highly sensitive 'losers' and others appear to be more resistant 'winners' that

© 2018 The Author(s) Published by the Royal Society. All rights reserved.

may potentially benefit from reduced competition for space or resources [8]. Differential sensitivities to Ω_{Ar} among coral species imply that ocean acidification has the potential to irrevocably alter coral assemblages for centuries to come. Despite this, little is known about how resistant species are better able to cope with acidification. Elevating pH (and thus $[CO_3^{2-}]$) at the internal site of calcification is one potential mechanism to maintain high Ω_{Ar} that may confer resistance [18–21], but the ability to raise pH is not limited to resistant species [22]. Alternatively, or in combination, corals could theoretically elevate internal Ca^{2+} to increase Ω_{Ar}, even though concentrations of Ca^{2+} in ambient seawater (approx. 10 mmol kg^{-1}) far exceed those of CO_3^{2-} (approx. 0.2 mmol kg^{-1}). The utility of elevating $[Ca^{2+}]$ is, however, potentially limited to less than a factor of approximately two increase relative to seawater because decreases in Mg/Ca will begin to favour the precipitation of calcite over aragonite [23] and the Ca^{2+}/CO_3^{2-} stoichiometry will become less optimal for crystal growth [24]. Nevertheless, while at least some corals can actively pump Ca^{2+} [25,26], no study has quantified changes in calcifying fluid Ca^{2+} ($[Ca^{2+}]_{cf}$) in response to seawater pH, and thus, the role of Ca^{2+} relative to CO_3^{2-} in defining resistance to ocean acidification remains unknown.

We apply a novel technique to derive $[Ca^{2+}]_{cf}$ in the corals *Acropora youngei* and *Pocillopora damicornis* cultured under simulated ocean acidification conditions. In the absence of direct or non-invasive techniques to measure $[Ca^{2+}]_{cf}$, we use the information provided by combining two recently developed geochemical proxies. First, the boron systematics ($\delta^{11}B$ and B/Ca) of aragonite quantify calcifying fluid carbonate chemistry, including pH_{cf} and $[CO_3^{2-}]_{cf}$ [27,28]. Second, Raman spectroscopy can be used to determine calcifying fluid Ω_{Ar} [29]. As Ω_{Ar} is a function of both $[CO_3^{2-}]$ and $[Ca^{2+}]$, boron systematics and Raman spectroscopy can be applied in tandem to derive $[Ca^{2+}]_{cf}$ (electronic supplementary material, table S1). Here, we use this approach to investigate the response of $[Ca^{2+}]_{cf}$ to seawater pH and its potential role in controlling the calcification sensitivity to ocean acidification.

2. Material and methods

The coral culturing experimental design was described previously by Comeau *et al*. [30]. Briefly, branches of *A. youngei* and *P. damicornis* were collected from Rottnest Island in Western Australia and transported to the Waterman's Bay experimental aquaria facility in Perth, Australia. The corals were allowed to recover for two weeks before exposure to treatments in 36 aquaria divided among three pH (total scale) treatments of 7.63, 7.81 and 8.09 maintained by CO_2 bubbling. After eight weeks, the apical tips of the skeletons were crushed to powders for geochemical and Raman analyses. B/Ca and $\delta^{11}B$ measurements and data are reported in Comeau *et al*. [30]. Mg/Ca and Sr/Ca ratios were measured on a Q-ICP-MS (X-series II, Thermo Fisher Scientific) following the methods of Holcomb *et al*. [31]. Precisions of Mg/Ca and Sr/Ca were 0.01 mmol mol^{-1} and 0.009 mmol mol^{-1}, respectively, based on repeated analyses of an in-house coral skeleton consistency standard.

Raman spectroscopy was conducted on the same powders used for geochemical analyses. Measurements were made on a WITec Alpha 300RA+ system with an Andor iDUS 401 CCD maintained at −60°C, and a 20× objective with 0.5 numerical aperture. An infrared (785 nm) laser was used with a 1200 mm^{-1} grating and the spectral centre placed at a Raman shift of 830 cm^{-1}. Coral skeleton powders were spread onto a glass slide and multiple grains (typically five) were sampled with 1 s integration times. A target for replication was set at 25 spectra per sample (i.e. per individual coral branch), although this was not always achieved as some spectra with poor signal (i.e. arbitrary intensity units less than 100) were subsequently filtered during data processing (electronic supplementary material, tables S2–S3). For each spectrum, the aragonite ν_1 peak was fit with a Gaussian curve, and the resulting full width at half maximum (FWHM) intensity was converted to Ω_{Ar} following the methods of DeCarlo *et al*. [29]. We note that Ω_{Ar} was estimated by Comeau *et al*. [30] based only on boron-derived $[CO_3^{2-}]_{cf}$ and assuming a constant $[Ca^{2+}]_{cf}$. Here, we use only the directly derived $[CO_3^{2-}]_{cf}$ from Comeau *et al*. [30], and instead, we calculate $[Ca^{2+}]_{cf}$ as follows:

$$[Ca^{2+}]_{cf} = \frac{\Omega_{Ar} * K_{sp}}{[CO_3^{2-}]_{cf}}, \tag{2.1}$$

where $[CO_3^{2-}]_{cf}$ and Ω_{Ar} are derived from boron systematics [28] and Raman spectroscopy, respectively. This equation is simply a rearrangement of the definition of aragonite saturation state shown in the Introduction. $Ca_{cf}^{2+}/Ca_{sw}^{2+}$ ratios were calculated by normalizing to $[Ca^{2+}]_{sw}$, which was estimated from salinity as 10.58 mmol kg^{-1} [32].

Precisions of derived $[Ca^{2+}]_{cf}$ were estimated with a Monte Carlo method. We repeated the calculation of $[Ca^{2+}]_{cf}$ 10^4 times, and in each iteration, we added random errors to the measured $\delta^{11}B$ (1σ analytical uncertainty of 0.17‰), B/Ca (1σ analytical uncertainty of 18 μmol mol^{-1}) and Raman FWHM (standard error of replicates per sample; electronic supplementary material, tables S2–S3), assuming Gaussian distributions. We estimated the 1σ uncertainty of $[Ca^{2+}]_{cf}$ by taking the standard deviation of the 10^4 Monte Carlo iterations.

We also tested whether our technique could be accurately applied to abiogenic (i.e. synthetic or inorganic) aragonites. These aragonites were precipitated from seawater with $[Ca^{2+}]$ manipulated by the addition of $CaCl_2$ and concentrated seawater [27], allowing us to check if our combined boron and Raman approach is sensitive to variations in $[Ca^{2+}]$. We used the seven abiogenic aragonite samples that were repeatedly analysed in DeCarlo *et al*. [29] for calibration of the Raman-Ω_{Ar} proxy, in addition to new Raman measurements on nine more abiogenic aragonite samples that were precipitated from fluids with $[Ca^{2+}]$ exceeding 12 mmol kg^{-1}, as described in [27]. Eight of the abiogenic aragonite samples were precipitated using a 'degassing' method in which $CaCO_3$ was dissolved in acidified seawater and precipitation occurred as the seawater pCO_2 equilibrated with the atmosphere. The degassing experiments were not used in calibrating the Raman-Ω_{Ar} proxy. The other eight experiments were conducted by pumping $Na_2CO_3/NaHCO_3$ solutions into filtered seawater. For each sample, we used the fluid pH, and the aragonite B/Ca and Raman FWHM to calculate $[Ca^{2+}]$ as described above. We then compared our derived $[Ca^{2+}]$ with that reported from measurements during the aragonite precipitation experiments [27].

Coral $[Ca^{2+}]_{cf}$ dynamics were separately estimated using Mg/Ca and Sr/Ca ratios of the coral skeletons. Coral calcification models that invoke seawater as the ultimate source of the calcifying fluid, Ca^{2+} addition to the fluid and precipitation from a closed or semi-closed reservoir have been successful at explaining much of the variability in the elemental composition of the skeleton [12,29,33,34]. Although such models have not been validated in terms of accurately predicting $[Ca^{2+}]_{cf}$ variability, they can provide insights into whether Ca^{2+} addition to the calcifying fluid is required to explain the skeletal geochemistry. We used the model described in [29] that predicts $[Ca^{2+}]_{cf}$ enrichment based on paired Mg/Ca and Sr/Ca data. The model is based on the abiogenic partitioning of these two element ratios between aragonite and seawater, and it solves for the combination of $[Ca^{2+}]_{cf}$ enrichment (which dilutes both Mg/Ca and

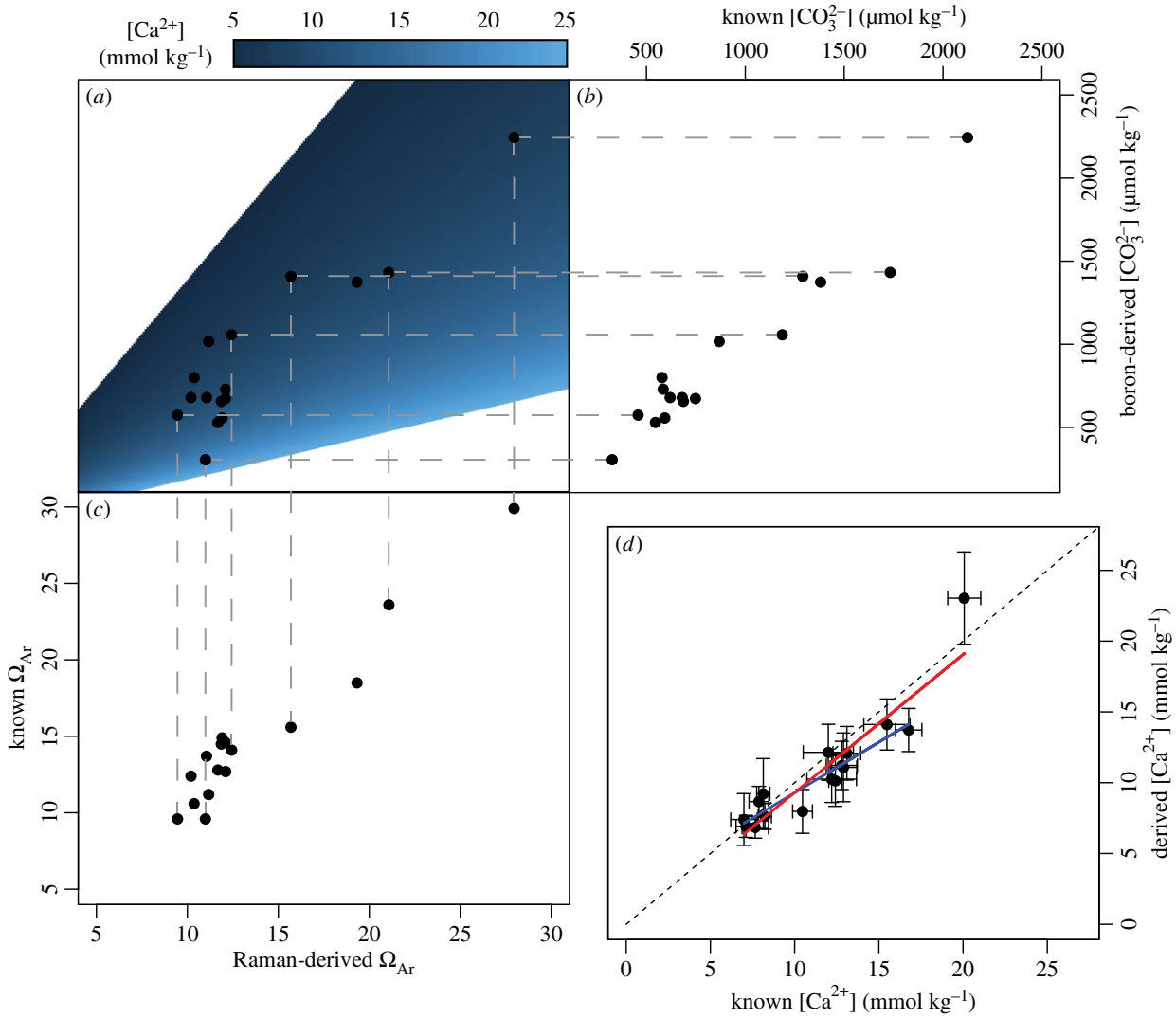

Figure 1. Test of deriving $[Ca^{2+}]$ from abiogenic aragonites precipitated under various Ca^{2+} concentrations. (*a*) Derived $[Ca^{2+}]$ (colours) as functions of Ω_{Ar} (*x*-axis) and $[CO_3^{2-}]$ (*y*-axis). Each black point shows the derived $[Ca^{2+}]$ of a separate abiogenic precipitation experiment. The boron-derived $[CO_3^{2-}]$ and Raman-derived Ω_{Ar} measurements that are used together to calculate $[Ca^{2+}]$ are shown in (*b*) and (*c*), respectively. The dashed grey lines each connect to the boron and Raman data from a single experiment, indicating how combining these data enables estimates of $[Ca^{2+}]$. For clarity, only a subset of these lines is plotted. (*d*) Comparison of derived $[Ca^{2+}]$ to the $[Ca^{2+}]$ known from fluid measurements during the aragonite precipitation experiments. The dashed black line indicates a 1 : 1 relationship, and the solid lines show regressions fit to all the data (red) and to all the data except the highest $[Ca^{2+}]$ point (blue). Error bars show 95% confidence intervals.

Sr/Ca) and Rayleigh fractionation (which increases Mg/Ca and decreases Sr/Ca) that match the measured element ratios. We performed two separate model runs: one in which addition to the calcifying fluid is 100% selective for Ca^{2+} and another in which addition is 50% 'leaky' with respect to Mg^{2+} and Sr^{2+} (i.e. $[Sr^{2+}]_{fluid} = (0.5Ca^{2+}_{addition})(Sr_{sw}/Ca_{sw}) + [Sr^{2+}]_{sw}$). Both produce the same patterns of variability, but the latter requires twice the $[Ca^{2+}]_{cf}$ enrichment to explain the measured element ratios.

All parameters ($[CO_3^{2-}]_{cf}$, $[Ca^{2+}]_{cf}$, Ω_{Ar}, calcification rate and modelled $[Ca^{2+}]_{cf}$) for each species were checked for normality with Kolmogorov–Smirnov tests and homogeneity of variances across pH treatments with Levene's tests. Regressions were performed using the linear model (*lm*) function in R [35] with species treated as factors as described in the text. Residuals of all regressions were also checked for normality with Kolmogorov–Smirnov tests.

3. Results and discussion

Our application of the Raman and boron proxies to the abiogenic aragonites produced $[Ca^{2+}]$ estimates that were correlated with the known $[Ca^{2+}]$ during the experiments (figure 1). A regression between derived and known $[Ca^{2+}]$ has a slope of 1.0 ± 0.1 ($r^2 = 0.82$) (figure 1*d*). Although excluding the highest $[Ca^{2+}]$ data point decreases the slope to 0.71 ± 0.09 ($r^2 = 0.82$), the data still indicate a sensitivity of the combined Raman–boron proxy to fluid $[Ca^{2+}]$. This result supports the overall reliability of our approach because the derived versus known $[Ca^{2+}]$ plot close to a 1 : 1 line, demonstrating that the Raman and B/Ca proxies differ primarily by their sensitivities to $[Ca^{2+}]$. The root-mean-square error of the derived to known $[Ca^{2+}]$ regression is 1.7 mmol kg^{-1}, and comparing this with the average standard deviation of derived $[Ca^{2+}]$ (0.9 mmol kg^{-1} for abiogenic data and 0.5 mmol kg^{-1} for our corals) indicates that at least half of the scatter in the regression is explained by propagation of errors from the boron and Raman measurements. That not all the scatter around the regression is accounted for by the propagated uncertainties may suggest that other factors have minor influences on either the boron or Raman proxies, but it is unlikely that we would be able to successfully reconstruct 82% the $[Ca^{2+}]$ variance of the

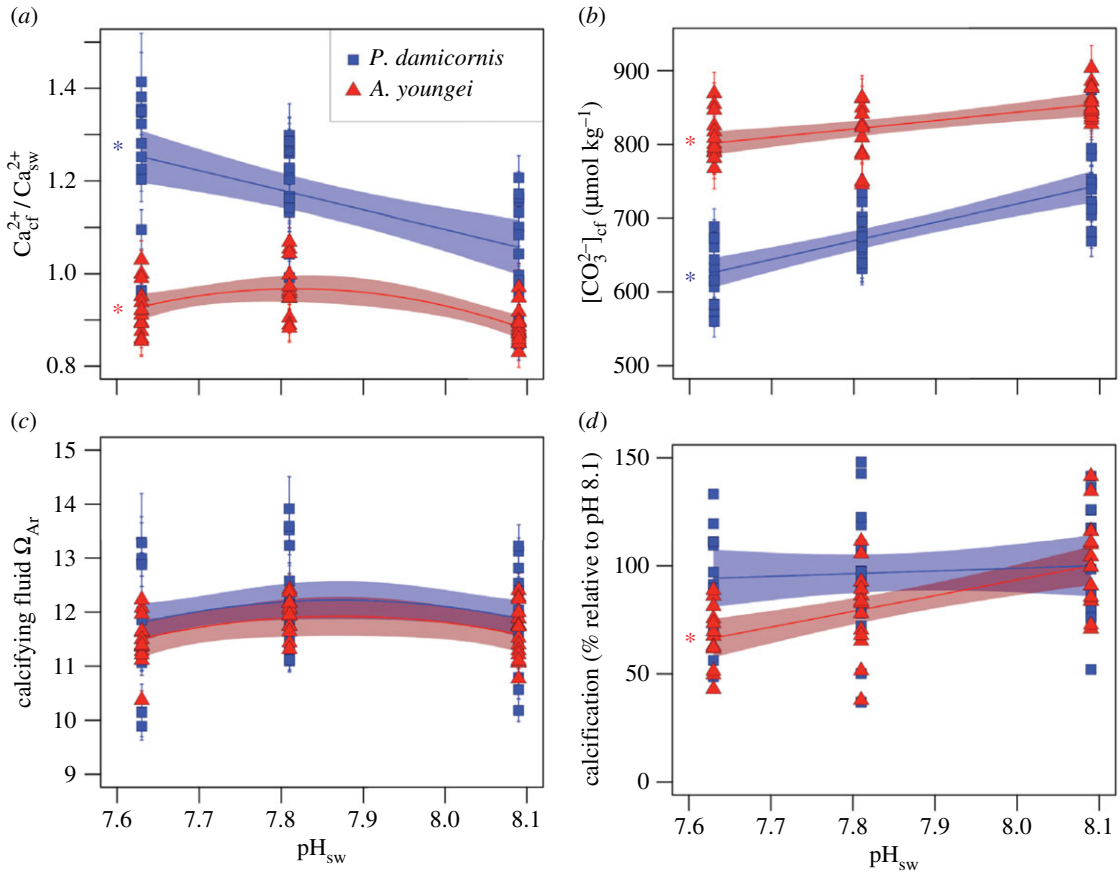

Figure 2. Sensitivity of calcifying fluid chemistry and calcification to seawater pH. (*a*) $Ca^{2+}_{cf}/Ca^{2+}_{sw}$, (*b*) $[CO_3^{2-}]_{cf}$, (*c*) Ω_{Ar} and (*d*) calcification responses to pH_{sw} treatments for both *P. damicornis* (blue squares) and *A. youngei* (red triangles). Bounded lines indicate regression fits $\pm$1 s.e. Coloured asterisks indicate which regressions are statistically significant ($p < 0.01$). Error bars on individual points represent 1 s.e.m.

experimental fluids if the primary controls of B/Ca and Raman FWHM were factors other than $[CO_3^{2-}]$ and Ω_{Ar}, respectively. Therefore, while each individual data point carries substantial uncertainty, our abiogenic test suggests that this approach is successful in capturing changes in $[Ca^{2+}]$ given suitable sample replication (figure 1).

In our culturing experiment, *P. damicornis* displayed a strong ability to control $[Ca^{2+}]_{cf}$, whereas *A. youngei* was unable to elevate $[Ca^{2+}]_{cf}$ in response to low pH. The ratio of $[Ca^{2+}]_{cf}$ to $[Ca^{2+}]$ of the external seawater ($Ca^{2+}_{cf}/Ca^{2+}_{sw}$) ranged from 0.85 to 1.41 for *P. damicornis* and increased significantly with decreasing seawater pH (pH_{sw}; $r^2 = 0.31$, $n = 42$, $p < 0.01$, $F_{1,40} = 19.3$; figure 2*a*). *Pocillopora damicornis* maintained $Ca^{2+}_{cf}/Ca^{2+}_{sw}$ of 1.06 ± 0.06 (s.e.) at present-day pH_{sw} (8.09), but it increased $Ca^{2+}_{cf}/Ca^{2+}_{sw}$ to 1.25 ± 0.06 at simulated end-of-century pH_{sw} (7.63) under a business-as-usual emissions scenario. Conversely, *A. youngei* did not consistently increase $Ca^{2+}_{cf}/Ca^{2+}_{sw}$ with decreasing pH_{sw}. Although *A. youngei* increased $Ca^{2+}_{cf}/Ca^{2+}_{sw}$ slightly from 0.89 ± 0.03 at the highest pH_{sw} to 0.97 ± 0.03 at the mid-pH_{sw} treatment, there was no further change in $Ca^{2+}_{cf}/Ca^{2+}_{sw}$ at the lowest pH_{sw} treatment (figure 2*a*). Calcifying fluid Ω_{Ar} was maintained at nearly constant levels across treatments for both species, with only slight declines at the lowest pH_{sw} (figure 2*c*). The ability of *P. damicornis* to control $[Ca^{2+}]_{cf}$ resulted in similar Ω_{Ar} compared with *A. youngei*, even though $[CO_3^{2-}]_{cf}$ was lower in *P. damicornis* (figure 2*b*) [30].

The species' differences in $Ca^{2+}_{cf}/Ca^{2+}_{sw}$ are mirrored in their calcification responses to acidification (figure 2*d*). While *A. youngei* calcification declined at lower pH_{sw} ($r^2 = 0.36$, $n = 42$, $p < 0.01$, $F_{1,40} = 24.3$), *P. damicornis* calcification was insensitive to pH_{sw} ($r^2 = 0.01$, $p = 0.58$). These contrasting responses appear to be driven not by calcifying fluid carbonate chemistry [30], but rather by $Ca^{2+}_{cf}/Ca^{2+}_{sw}$. In fact, $[CO_3^{2-}]_{cf}$ was significantly more sensitive to pH_{sw} for *P. damicornis* than for *A. youngei* ($r^2 = 0.83$, $n = 84$, $p < 0.01$, $F_{3,80} = 134.9$), contrasting their calcification sensitivities to pH_{sw} (figure 2). Similarly, *P. damicornis* calcification has been shown to be insensitive to acidification across multiple locations in the Pacific Ocean [36], whereas *A. youngei* is highly sensitive [37,38]. Although the mechanisms underlying these different sensitivities have so far remained largely unresolved, our results suggest that resistant corals are those with the ability to elevate $[Ca^{2+}]_{cf}$, and more susceptible species are those which cannot.

There are two non-mutually exclusive hypotheses to explain the changes in $Ca^{2+}_{cf}/Ca^{2+}_{sw}$ that we observed: (i) passive precipitation of $CaCO_3$ and (ii) active upregulation by the coral polyps. Mass balance considerations imply that accretion of $CaCO_3$ skeleton consumes $[Ca^{2+}]_{cf}$, but this does not exclude the possibility that upregulation of processes controlling $[Ca^{2+}]_{cf}$ is also involved. Indeed, several lines of evidence support that much of the $Ca^{2+}_{cf}/Ca^{2+}_{sw}$ variability in our experiment was driven by the activity of the corals. First, while there is a weak inverse correlation between $Ca^{2+}_{cf}/Ca^{2+}_{sw}$ and calcification when data for both species are combined ($r^2 = 0.22$, $n = 84$, $p < 0.01$, $F_{1,82} = 24.0$), there are no significant correlations within each species (figure 3*a*). Second, the $Ca^{2+}_{cf}/Ca^{2+}_{sw}$ exceeding 1 for *P. damicornis* cannot be explained by $CaCO_3$ precipitation and requires some

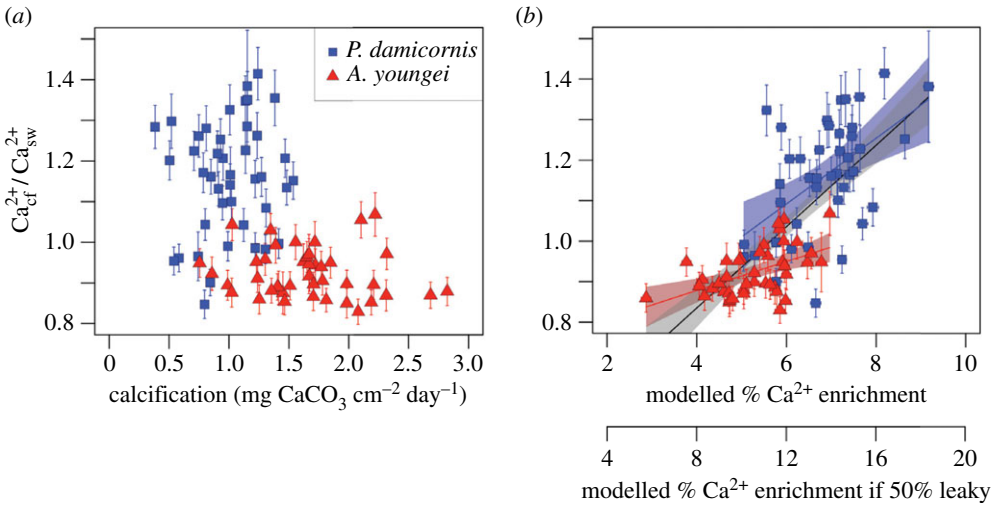

Figure 3. Factors driving $Ca^{2+}_{cf}/Ca^{2+}_{sw}$ variability. Sensitivity of $Ca^{2+}_{cf}/Ca^{2+}_{sw}$ to (*a*) calcification and (*b*) $[Ca^{2+}]_{cf}$ elevation estimated by modelling with Mg/Ca and Sr/Ca ratios. In (*b*), the upper *x*-axis values show the model assuming 100% selectivity for Ca^{2+}, and the lower *x*-axis values show the model that is 50% leaky with respect to Mg^{2+} and Sr^{2+} ions. The black line with grey error bound in (*b*) corresponds to regressions fit to the data from both species. The coloured lines and error bounds in (*b*) show species-specific regressions. Colours are the same as in figure 2.

mechanism of increasing $[Ca^{2+}]_{cf}$. Finally, we independently estimated $[Ca^{2+}]_{cf}$ using skeletal Mg/Ca and Sr/Ca ratios and a simple model [29] in which these element/Ca ratios are explained by initial $[Ca^{2+}]_{cf}$ elevation followed by precipitation from a closed reservoir. The elevation of $[Ca^{2+}]_{cf}$ estimated from this modelling exercise is strongly correlated ($r^2 = 0.53$, $n = 84$, $p < 0.01$, $F_{1,82} = 93.0$) with our derived $Ca^{2+}_{cf}/Ca^{2+}_{sw}$ ratios, and significant positive correlations are found within each species (figure 3*b*). However, the model implies that $[Ca^{2+}]_{cf}$ is elevated up to 10% with respect to seawater, which is less than the upper limit of 25% indicated by our maximum derived mean $Ca^{2+}_{cf}/Ca^{2+}_{sw}$ of 1.25 for *Pocillopora* at the lowest pH_{sw}. One possible reason for this is that the model assumes that the addition of Ca^{2+} to the calcifying fluid is 100% selective for Ca^{2+}. Allowing this process to be partially leaky with respect to Sr^{2+} and Mg^{2+} ions [39] brings the modelled $[Ca^{2+}]_{cf}$ elevation into closer agreement with our derived $Ca^{2+}_{cf}/Ca^{2+}_{sw}$ (figure 3*b*). Transporting Mg^{2+} along with Ca^{2+} to the calcifying fluid may allow $[Ca^{2+}]_{cf}$ to be elevated without favouring calcite growth over aragonite. Further geochemical evidence for active $[Ca^{2+}]_{cf}$ elevation comes from calcium isotope ratios in modern and fossil coral skeletons, which cannot be reconciled with direct precipitation from seawater [40,41]. Rather, the calcium isotopic offset between coral skeletons and seawater supports strong biological modulation of $[Ca^{2+}]_{cf}$ [40] and potentially some effects of Rayleigh fractionation or Ca^{2+} diffusion between the calcifying fluid and the external environment [41].

Corals may influence their $[Ca^{2+}]_{cf}$ via multiple mechanisms. These potentially include Ca-channels [25,39,42–44], Ca^{2+}/Na^{+} exchange [43], Ca^{2+}-ATPase [26] and precipitation/dissolution of amorphous $CaCO_3$ [45]. The only previous measurements of coral $[Ca^{2+}]_{cf}$ were made by cutting an incision in living *Galaxea fascicularis* polyps and inserting a Ca^{2+} microsensor near the skeleton surface [26]. Although potentially invasive, these previous data showed elevation above seawater concentrations by up to 10%, within the range of our $Ca^{2+}_{cf}/Ca^{2+}_{sw}$ ratios. Importantly, the microsensor data allowed for continuous measurements, which revealed a strong sensitivity of $[Ca^{2+}]_{cf}$ to light, likely because the polyp uses energy provided by its photosynthetic symbionts to drive the activity of various Ca^{2+}-transport mechanisms [26,44]. In additional laboratory experiments that exposed corals to Ca-channel and Ca^{2+}-ATPase inhibitors, $[Ca^{2+}]_{cf}$ variability was dampened and calcification rates were decreased [26,39,43]. These multiple lines of evidence make it clear that some corals have cellular mechanisms in place to modulate $[Ca^{2+}]_{cf}$, and our results demonstrate that resistant species such as *Pocillopora* can upregulate these processes to resist the effects of ocean acidification and to maintain normal calcification rates even at low pH_{sw}. Conversely, our data indicate that *A. youngei* exerts less control on $[Ca^{2+}]_{cf}$, consistent with a previous experiment that found gene expression for ion transporters in *Acropora* did not change in response to seawater pH [46].

Our unique characterization of $[CO_3^{2-}]_{cf}$ and $[Ca^{2+}]_{cf}$ enables the first evaluation of their relative influences on calcifying fluid Ω_{Ar}. Most models of coral calcification rely on the assumption that Ω_{Ar} is controlled by $[CO_3^{2-}]_{cf}$ and that variability in $[Ca^{2+}]_{cf}$ is negligible [20,47]. However, we found no significant correlations between $[CO_3^{2-}]_{cf}$ and Ω_{Ar}, neither within nor between species (figure 4*a*). Rather, Ω_{Ar} is positively correlated ($r^2 = 0.47$, $n = 84$, $p < 0.01$, $F_{2,81} = 37.8$) with $[Ca^{2+}]_{cf}$ for both *A. youngei* and *P. damicornis* (figure 4*b*). This finding should, however, be viewed with some caution because our technique of deriving $[Ca^{2+}]_{cf}$ in part from proxy measurements of Ω_{Ar} means that they are not independent, and thus, it is difficult to determine if this correlation represents a causal relationship. Nevertheless, for a given $[Ca^{2+}]_{cf}$, calcifying fluid Ω_{Ar} is higher in *A. youngei* than *P. damicornis*, which may explain the overall faster calcification of *A. youngei* [30]. Critically though, $[Ca^{2+}]_{cf}$ for *A. youngei* remains within a relatively narrow range, whereas *P. damicornis* is capable of driving Ω_{Ar} higher, potentially by elevating $[Ca^{2+}]_{cf}$. This ability may account for the relative insensitivity of *P. damicornis* calcification to seawater pH, although we cannot exclude some influence of other factors such as changes in calcifying time or surface area within the calyx.

Ocean acidification, combined with warming, threatens to disrupt coral growth and survival [6–8,38]. Although some resistant species are likely to persist, the differential responses

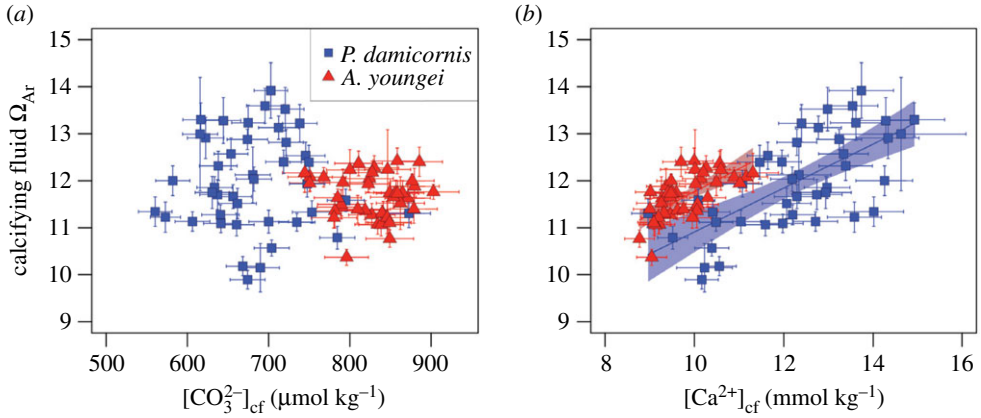

Figure 4. Relative influences on coral calcifying fluid Ω_{Ar}. Sensitivity of Ω_{Ar} to (*a*) $[CO_3^{2-}]_{cf}$ and (*b*) $[Ca^{2+}]_{cf}$. Colours are the same as in figure 2.

to ocean acidification will potentially create novel configurations of species occupying coral reefs. If coral communities shift in favour of species resistant to ocean acidification [8], there are likely to be cascading effects in reef ecosystems due to the associations of other reef biota with the habitat created by susceptible coral genera such as *Acropora* [48]. Furthermore, declines in $CaCO_3$ production by susceptible genera are expected to be exacerbated by increasing bioerosion and carbonate dissolution rates as seawater pH declines [49–53]. In tandem, these changes in $CaCO_3$ budgets could inhibit some reefs from keeping pace with rising sea levels [54]. Identifying which corals can cope with ocean acidification by increasing $[Ca^{2+}]_{cf}$ provides a new perspective in identifying more resistant species, which may help efforts to forecast the changing state and viability of coral reefs as anthropogenic CO_2 continues to invade the oceans.

Ethics. All local regulations and permit requirements were followed during this study.

Data accessibility. Datasets supporting this article have been uploaded as the electronic supplementary material, and the raw data and code are available at https://codeocean.com/2018/03/12/code-for-amp-num-34-semi-resistant-corals-increase-calcium-to-cope-with-ocean-acidification-amp-num-34-semi/code.

Authors' contributions. S.C. and C.E.C. performed the culturing experiments and measured the skeletal geochemistry. T.M.D. performed the Raman analyses, designed the technique for quantifying calcium concentrations, and wrote the manuscript. All authors contributed to interpreting data and editing the manuscript.

Competing interests. The authors declare that they have no competing interests.

Funding. This study was funded by an ARC Laureate Fellowship (FL120100049) awarded to M.T.M., the ARC Centre of Excellence for Coral Reef Studies (CE140100020) and S.C. was supported by an ARC DECRA (DE160100668).

Acknowledgements. Thomas Becker (CMCA) assisted with Raman spectroscopy measurements. The authors acknowledge the facilities and the scientific and technical assistance of the Australian Microscopy & Microanalysis Research Facility at the Centre for Microscopy, Characterisation and Analysis, The University of Western Australia, a facility funded by the University, State and Commonwealth Governments. J. Ries and one anonymous reviewer provided helpful comments that improved the quality of a previous version of this manuscript.

References

1. IPCC. 2013 Climate change 2013: the physical science basis. *Contribution of Working Group I to the Fifth Assessment Report of the Intergovernmental Panel on Climate Change* (eds TF Stocker *et al.*), pp. 1535. Cambridge, UK: Cambridge University Press.
2. Tyrrell T, Zeebe RE. 2004 History of carbonate ion concentration over the last 100 million years. *Geochim. Cosmochim. Acta* **68**, 3521–3530. (doi:10.1016/j.gca.2004.02.018)
3. Hönisch B *et al.* 2012 The geological record of ocean acidification. *Science* **335**, 1058–1063. (doi:10.1126/science.1208277)
4. Zeebe RE, Ridgwell A, Zachos JC. 2016 Anthropogenic carbon release rate unprecedented during the past 66 million years. *Nat. Geosci.* **9**, 325–329. (doi:10.1038/ngeo2681)
5. Sabine CL *et al.* 2004 The oceanic sink for anthropogenic CO_2. *Science* **305**, 367–371. (doi:10.1126/science.1097403)
6. Hoegh-Guldberg O *et al.* 2007 Coral reefs under rapid climate change and ocean acidification. *Science* **318**, 1737–1742. (doi:10.1126/science.1152509)
7. De'ath G, Lough JM, Fabricius KE. 2009 Declining coral calcification on the Great Barrier Reef. *Science* **323**, 116. (doi:10.1126/science.1165283)
8. Fabricius KE *et al.* 2011 Losers and winners in coral reefs acclimatized to elevated carbon dioxide concentrations. *Nat. Clim. Chang.* **1**, 165–169. (doi:10.1038/nclimate1122)
9. IPCC. 2014 Climate Change 2014: Impacts, adaptation, and vulnerability. Part B: regional aspects. *Contribution of Working Group II to the Fifth Assessment Report of the Intergovernmental Panel on Climate Change* (eds V Barros *et al.*), pp. 688. Cambridge, UK: Cambridge University Press.
10. Barnes DJ. 1970 Coral skeletons: an explanation of their growth and structure. *Science* **170**, 1305–1308. (doi:10.1126/science.170.3964.1305)
11. Clode PL, Marshall AT. 2002 Low temperature FESEM of the calcifying interface of a scleractinian coral. *Tissue Cell* **34**, 187–198. (doi:10.1016/S0040-8166(02)00031-9)
12. Gagnon AC, Adkins JF, Erez J. 2012 Seawater transport during coral biomineralization. *Earth Planet. Sci. Lett.* **329**, 150–161. (doi:10.1016/j.epsl.2012.03.005)
13. Burton EA, Walter LM. 1987 Relative precipitation rates of aragonite and Mg calcite from seawater: Temperature or carbonate ion control? *Geology* **15**, 111–114. (doi:10.1130/0091-7613(1987)15<111:RPROAA>2.0.CO;2)
14. Gattuso J-P, Frankignoulle M, Bourge I, Romaine S, Buddemeier RW. 1998 Effect of calcium carbonate saturation of seawater on coral calcification. *Glob. Planet. Change* **18**, 37–46. (doi:10.1016/S0921-8181(98)00035-6)
15. Langdon C, Takahashi T, Sweeney C, Chipman D, Goddard J, Marubini F, Aceves H, Barnett H, Atkinson MJ. 2000 Effect of calcium carbonate saturation state on the calcification rate of an experimental coral reef. *Glob. Biogeochem. Cycles* **14**, 639–654. (doi:10.1029/1999GB001195)
16. Chan NCS, Connolly SR. 2013 Sensitivity of coral calcification to ocean acidification: a meta-analysis.

Glob. Chang. Biol. **19**, 282–290. (doi:10.1111/gcb.12011)

17. Swart PK. 1979 The effect of seawater calcium concentrations on the growth and skeletal composition of a scleractinian coral: *Acropora squamosa*. *SEPM J. Sediment. Res.* **49**, 951–954. (doi:10.1306/212F7888-2B24-11D7-8648000 102C1865D)
18. Wall M, Fietzke J, Schmidt GM, Fink A, Hofmann LC, de Beer D, Fabricius KE. 2016 Internal pH regulation facilitates *in situ* long-term acclimation of massive corals to end-of-century carbon dioxide conditions. *Sci. Rep.* **6**, 30688. (doi:10.1038/srep30688)
19. Ries JB, Cohen AL, McCorkle DC. 2009 Marine calcifiers exhibit mixed responses to CO_2-induced ocean acidification. *Geology* **37**, 1131. (doi:10.1130/G30210A.1)
20. Ries JB. 2011 A physicochemical framework for interpreting the biological calcification response to CO_2-induced ocean acidification. *Geochim. Cosmochim. Acta* **75**, 4053–4064. (doi:10.1016/j.gca.2011.04.025)
21. Venn A, Tambutte E, Holcomb M, Allemand D, Tambutte S. 2011 Live tissue imaging shows reef corals elevate pH under their calcifying tissue relative to seawater. *PLoS ONE* **6**, e20013. (doi:10.1371/journal.pone.0020013)
22. McCulloch MT, Falter J, Trotter J, Montagna P. 2012 Coral resilience to ocean acidification and global warming through pH up-regulation. *Nat. Clim. Chang.* **2**, 623–627. (doi:10.1038/nclimate1473)
23. Ries JB, Stanley SM, Hardie LA. 2006 Scleractinian corals produce calcite, and grow more slowly, in artificial Cretaceous seawater. *Geology* **34**, 525. (doi:10.1130/G22600.1)
24. Nehrke G, Reichart G, Van Cappellen P, Meile C, Bijma J. 2007 Dependence of calcite growth rate and Sr partitioning on solution stoichiometry: non-Kossel crystal growth. *Geochim. Cosmochim. Acta* **71**, 2240–2249. (doi:10.1016/J.GCA.2007.02.002)
25. Zoccola D, Tambutté E, Sénégas-Balas F, Michiels J-F, Failla J-P, Jaubert J, Allemand D. 1999 Cloning of a calcium channel α1 subunit from the reef-building coral, *Stylophora pistillata*. *Gene* **227**, 157–167. (doi:10.1016/S0378-1119(98)00602-7)
26. Al-Horani FA, Al-Moghrabi SM, De Beer D. 2003 The mechanism of calcification and its relation to photosynthesis and respiration in the scleractinian coral *Galaxea fascicularis*. *Mar. Biol.* **142**, 419–426. (doi:10.1007/s00227-002-0981-8)
27. Holcomb M, DeCarlo TM, Gaetani GA, McCulloch M. 2016 Factors affecting B/Ca ratios in synthetic aragonite. *Chem. Geol.* **437**, 67–76. (doi:10.1016/j.chemgeo.2016.05.007)
28. McCulloch MT, D'Olivo Cordero JP, Falter J, Holcomb M, Trotter JA. 2017 Coral calcification in a changing world: the interactive dynamics of pH and DIC up-regulation. *Nat. Commun.* **8**, 15686. (doi:10.1038/ncomms15686)
29. DeCarlo TM, D'Olivo JP, Foster T, Holcomb M, Becker T, McCulloch MT. 2017 Coral calcifying fluid aragonite saturation states derived from Raman spectroscopy. *Biogeosciences* **14**, 5253–5269. (doi:10.5194/bg-14-5253-2017)
30. Comeau S, Cornwall CE, McCulloch MT. 2017 Decoupling between the response of coral calcifying fluid pH and calcification to ocean acidification. *Sci. Rep.* **7**, 7573. (doi:10.1038/s41598-017-08003-z)
31. Holcomb M, DeCarlo TM, Schoepf V, Dissard D, Tanaka K, McCulloch M. 2015 Cleaning and pre-treatment procedures for biogenic and synthetic calcium carbonate powders for determination of elemental and boron isotopic compositions. *Chem. Geol.* **398**, 11–21. (doi:10.1016/j.chemgeo.2015.01.019)
32. Riley JP, Tongudai M. 1967 The major cation/chlorinity ratios in sea water. *Chem. Geol.* **2**, 263–269. (doi:10.1016/0009-2541(67)90026-5)
33. Gaetani GA, Cohen AL. 2006 Element partitioning during precipitation of aragonite from seawater: a framework for understanding paleoproxies. *Geochim. Cosmochim. Acta* **70**, 4617–4634. (doi:10.1016/j.gca.2006.07.008)
34. DeCarlo TM, Gaetani GA, Holcomb M, Cohen AL. 2015 Experimental determination of factors controlling U/Ca of aragonite precipitated from seawater: implications for interpreting coral skeleton. *Geochim. Cosmochim. Acta* **162**, 151–165. (doi:10.1016/j.gca.2015.04.016)
35. R Core Team. 2016 *R: a language and environment for statistical computing*. Vienna, Austria: R Foundation for Statistical Computing.
36. Comeau S, Carpenter RC, Nojiri Y, Putnam HM, Sakai K, Edmunds PJ. 2014 Pacific-wide contrast highlights resistance of reef calcifiers to ocean acidification. *Proc. R. Soc. B* **281**, 20141339. (doi:10.1098/rspb.2014.1339)
37. Schneider K, Erez J. 2006 The effect of carbonate chemistry on calcification and photosynthesis in the hermatypic coral *Acropora eurystoma*. *Limnol. Oceanogr.* **51**, 1284–1293. (doi:10.4319/lo.2006.51.3.1284)
38. Anthony KRN, Kline DI, Diaz-Pulido G, Dove S, Hoegh-Guldberg O. 2008 Ocean acidification causes bleaching and productivity loss in coral reef builders. *Proc. Natl Acad. Sci. USA* **105**, 17 442–17 446. (doi:10.1073/pnas.0804478105)
39. Allison N, Cohen I, Finch AA, Erez J, EIMF F. 2011 Controls on Sr/Ca and Mg/Ca in scleractinian corals: the effects of Ca–ATPase and transcellular Ca channels on skeletal chemistry. *Geochim. Cosmochim. Acta* **75**, 6350–6360. (doi:10.1016/j.gca.2011.08.012)
40. Inoue M, Gussone N, Koga Y, Iwase A, Suzuki A, Sakai K, Kawahata H. 2015 Controlling factors of Ca isotope fractionation in scleractinian corals evaluated by temperature, pH and light controlled culture experiments. *Geochim. Cosmochim. Acta* **167**, 80–92. (doi:10.1016/j.gca.2015.06.009)
41. Gothmann AM, Bender ML, Blättler CL, Swart PK, Giri SJ, Adkins JF, Stolarski J, Higgins JA. 2016 Calcium isotopes in scleractinian fossil corals since the Mesozoic: implications for vital effects and biomineralization through time. *Earth Planet. Sci. Lett.* **444**, 205–214. (doi:10.1016/j.epsl.2016.03.012)
42. Allemand D, Ferrier-Pagès C, Furla P, Houlbrèque F, Puverel S, Reynaud S, Tambutté É, Tambutté S, Zoccola D. 2004 Biomineralisation in reef-building corals: from molecular mechanisms to environmental control. *C. R. Palevol* **3**, 453–467. (doi:10.1016/j.crpv.2004.07.011)
43. Marshall AT. 1996 Calcification in hermatypic and ahermatypic corals. *Science* **271**, 637–640. (doi:10.1126/science.271.5249.637)
44. Marshall AT, Clode PL, Russell R, Prince K, Stern R. 2007 Electron and ion microprobe analysis of calcium distribution and transport in coral tissues. *J. Exp. Biol.* **210**, 2443–2463. (doi:10.1242/jeb.003343)
45. Mass T *et al.* 2017 Amorphous calcium carbonate particles form coral skeletons. *Proc. Natl Acad. Sci. USA* **114**, E7670–E7678. (doi:10.1073/pnas.1707890114)
46. Moya A *et al.* 2012 Whole transcriptome analysis of the coral *Acropora millepora* reveals complex responses to CO_2-driven acidification during the initiation of calcification. *Mol. Ecol.* **21**, 2440–2454. (doi:10.1111/j.1365-294X.2012.05554.x)
47. Allison N, Cohen I, Finch AA, Erez J, Tudhope AW. 2014 Corals concentrate dissolved inorganic carbon to facilitate calcification. *Nat. Commun.* **5**, 5741. (doi:10.1038/ncomms6741)
48. Bonin MC. 2012 Specializing on vulnerable habitat: acropora selectivity among damselfish recruits and the risk of bleaching-induced habitat loss. *Coral Reefs* **31**, 287–297. (doi:10.1007/s00338-011-0843-2)
49. Wisshak M, Schönberg CHL, Form A, Freiwald A. 2012 Ocean acidification accelerates reef bioerosion. *PLoS ONE* **7**, e45124. (doi:10.1371/journal.pone.0045124)
50. Silbiger NJ, Guadayol O, Thomas FIM, Donahue MJ. 2014 Reefs shift from net accretion to net erosion along a natural environmental gradient. *Mar. Ecol. Prog. Ser.* **515**, 33–44. (doi:10.3354/meps10999)
51. DeCarlo TM, Cohen AL, Barkley HC, Cobban Q, Young C, Shamberger KE, Brainard RE, Golbuu Y. 2015 Coral macrobioerosion is accelerated by ocean acidification and nutrients. *Geology* **43**, 7–10. (doi:10.1130/G36147.1)
52. Schönberg CHL, Fang JKH, Carreiro-Silva M, Tribollet A, Wisshak M. 2017 Bioerosion: the other ocean acidification problem. *ICES J. Mar. Sci.* **74**, 895–925. (doi:10.1093/icesjms/fsw254)
53. Ries JB, Ghazaleh MN, Connolly B, Westfield I, Castillo KD. 2016 Impacts of seawater saturation state ($\Omega_A = 0.4–4.6$) and temperature (10, 25°C) on the dissolution kinetics of whole-shell biogenic carbonates. *Geochim. Cosmochim. Acta* **192**, 318–337. (doi:10.1016/J.GCA.2016.07.001)
54. Yates KK, Zawada DG, Smiley NA, Tiling-Range G. 2017 Divergence of seafloor elevation and sea level rise in coral reef ecosystems. *Biogeosciences* **14**, 1739–1772. (doi:10.5194/bg-14-1739-2017)